Available online at www.sciencedirect.com

SciVerse ScienceDirect

Ceramics International 38 (2012) 3129–3134

CERAMICS INTERNATIONAL

www.elsevier.com/locate/ceramint

# The optical properties of Ti-doped $TiO_2$ nanoceramic films deposited by simultaneous rf and dc magnetron sputtering

Su-Shia Lin *

*Department of Applied Materials and Optoelectronic Engineering, National Chi Nan University, Puli, Nantou Hsien 54561, Taiwan, ROC*

Received 14 November 2011; accepted 6 December 2011
Available online 14 December 2011

**Abstract**

The Ti-doped $TiO_2$ ($TiO_2$:Ti) nanoceramic films were deposited by simultaneous rf magnetron sputtering of $TiO_2$ and dc magnetron sputtering of Ti. When dc power increased, TiO preferentially formed and the deposited films had lower O/Ti atomic ratio, especially at low substrate temperature. With the decrease of substrate temperature, the $TiO_2$:Ti film had relatively high optical energy gap, therefore the absorption edge showed the blue shift. The nonlinear refractive indices of $TiO_2$:Ti films prepared at different dc powers and substrate temperatures were measured by Moiré deflectometry, and were of the order of $10^{-8}$ $cm^2$ $W^{-1}$. By decreasing dc power and increasing substrate temperature, $TiO_2$:Ti film exhibited lower surface roughness, higher linear refractive index and lower stress-optical coefficient.


*Keywords:* Films; Sputtering; Power; Substrate temperature; Optical energy gap; Refractive index

## 1. Introduction

Titanium dioxide ($TiO_2$) films have attracted much attention in various fields such as insulators of metal-oxide-semiconductor field effect transistor [1], electrodes for solar energy conversion [2] and photocatalysts [3], because of their high dielectric constant and appropriate semiconducting properties. $TiO_2$ is also a very popular material for optical and protective applications because of its high transparency in the visible region [4] and excellent mechanical durability. Doped films generally can be caused to have very stable optical properties [5].

The characteristics of films are affected by the preparation conditions such as working pressure, substrate temperature, types of substrates, and the thickness of the films [6]. In this study, Ti-doped $TiO_2$ ($TiO_2$:Ti) nanoceramic films were prepared by simultaneous rf magnetron sputtering of $TiO_2$ and dc magnetron sputtering of Ti. The advantages of sputtering are the simplicity of the apparatus, high deposition rate, good surface flatness, and high density of the deposited layer [7]. The influence of dc power and substrate temperature on the optical properties of $TiO_2$:Ti nanoceramic films was investigated.

Transparent materials generally exhibit the optical Kerr effect. The nonlinear refractive indices of materials are of great interest because of potential applications in designing optical devices and laser technology [8–11]. Moiré deflectometry is a powerful tool for measuring the nonlinear refractive indices of materials. The main advantages of the Moiré deflectometry technique are its extreme experimental simplicity, lower cost and lower sensitivity to external disturbances than other interferometric methods. In this study, this method is applied to measure the nonlinear refractive indices of $TiO_2$:Ti films on glass substrates under illumination with a 5 mW He–Ne laser ($\lambda$ = 632.8 nm).

## 2. Experimental procedures

The $TiO_2$:Ti nanoceramic films were deposited on glass (Corning 1737) by simultaneous rf magnetron sputtering of $TiO_2$ and dc magnetron sputtering of Ti. The dimension of the glass substrates was 24 mm × 24 mm × 1.1 mm. Before deposition, the substrates were ultrasonically cleaned in alcohol, rinsed in deionized water and dried in nitrogen. Two circular targets were used (5 cm diameter, 5 mm thickness); the first was sintered stoichiometric $TiO_2$ (99.99% purity); the other was metallic Ti (99.999% purity).

* Tel.: +886 49 2910960x4771; fax: +886 49 2912238.
*E-mail address:* sushia@ncnu.edu.tw.

0272-8842/$36.00 
doi:10.1016/j.ceramint.2011.12.014

The sputtering was performed in an Ar atmosphere with a target-to-substrate distance of 15 cm. A turbo-molecular pump, backed by a rotary pump, was used to achieve a base pressure of $1.3 \times 10^{-4}$ Pa. For the deposition of the films, the substrate temperature was controlled in the range of 100–500 °C. The working pressure was 1.5 Pa. An rf power (13.56 MHz, RGN CONTROLLER, ULVAC, Japan) of 50 W was supplied to the $TiO_2$ target, and a dc power (DCS0052B, ULVAC, Japan) of 5–9 W was applied to the Ti target. No external bias voltage was applied to substrate. The rotating speed of the substrate was 20 rpm, and the thickness of films was maintained at 100 nm.

The film thickness was measured using a surface profiler (Alpha-Step 500, TENCOR, Santa Clara, CA). The elemental compositions were investigated by X-ray photoemission spectroscopy (XPS; PHI 5000 VersaProbe, Japan). The surface morphologies and surface roughness were examined by atomic force microscopy (AFM; Digital Instruments Inc., NanoScope E, USA). The optical transmission spectra of films in the ultraviolet–visible–infrared (UV–vis–IR) region were obtained using a spectrophotometer (HP 8452A diode array spectrophotometer, Hewlett Packard, Palo Alto, CA). The linear refractive indices of films were recorded using a spectrometer (MP100-ST, Fremont, CA). The stress was measured by Nano Indenter XP System (MTS Systems Corporation, MN USA).

Fig. 1 shows the Moiré deflectometry experimental set-up that is used to measure the nonlinear refractive indices of $TiO_2$:Ti films on glass substrates. Lens $L_1$ focused a 5 mW He–Ne laser beam (wavelength of 632.8 nm), which was re-collimated by lens $L_2$. The focal lengths of lenses $L_1$, $L_2$ and $L_3$ were 100, 200 and 200 mm, respectively. Two similar Ranchi gratings $G_1$ and $G_2$ with a pitch of 0.1 mm were used to construct the Moiré fringe patterns. The distance between the planes of $G_1$ and $G_2$ was set to 64 mm, which is one of the Talbot distances of the used gratings. The Talbot distances satisfy $z_t = tp^2/\lambda$ where $p$ is the periodicity of the grating; $\lambda$ is the wavelength of light; $t$ is an integer. In this work, the Moiré fringes were clearly formed for a Talbot distance of $z_{t=4} \approx 64$ mm, indicating that the Moiré fringes were observed on a screen attached to the second grating. The Moiré fringe patterns were projected onto a computerized CCD camera by lens $L_3$, which was placed at the back of the second grating.

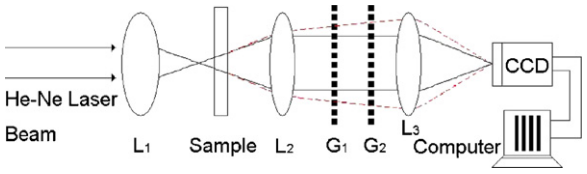


Fig. 1. The experimental set-up for measuring index of nonlinear refraction by Moiré deflectometry technique.

## 3. Results and discussion

### 3.1. Film composition

Table 1 shows the deposition rate and elemental composition of $TiO_2$:Ti films under different sputtering conditions. The deposition rate increased with dc power, and increased with the decrease of the substrate temperature. When the dc power increased, the particles of generation by sputtering and the probability of the particles arriving at the substrate increased, therefore the deposition rate increased [12]. However, the diffusive ability of atoms or molecules increased with the increase of substrate temperature, which resulted in lower deposition rate [13]. The elemental composition of $TiO_2$:Ti films were analyzed by XPS. The O/Ti atomic ratio increased with decreasing dc power and increasing substrate temperature, suggesting that the deposited films became more stoichiometric when dc power decreased and substrate temperature increased.

Fig. 2 shows O 1s photoelectron peak in the XPS spectrum of $TiO_2$:Ti films prepared at different dc powers and substrate temperatures. The peaks at 530.1 and 531.2 eV correspond to oxygen in TiO and $TiO_2$ [14]. The peak shifted to near bonding energy of 530.1 eV with increasing dc power, indicating that TiO formed preferentially when dc power increased. However, no obvious shift of peak was found with increasing substrate temperature. The O 1s photoelectron peak demonstrates a binding energy shift with changing dc power.

Fig. 3 shows the morphologies of $TiO_2$:Ti films deposited under different conditions. For $TiO_2$:Ti films deposited under different dc powers and substrate temperatures, uniform grains with island structure were observed. By comparing Fig. 3a with c and b with d, the roughness increased with dc power. It was probably due to metallic titanium present, as interstitial atoms in the lattice of $TiO_2$ nanocrystallites in the film [15].

By comparing Fig. 3a with b and c with d, the $TiO_2$:Ti films had lower roughness at high substrate temperature. The collisions of these particles with the growing film could smooth the thin film by surface diffusion mechanism and enhanced surface atom mobility [13,16]. Because the probability of collisions of particles increased with substrate temperature, it is probably why $TiO_2$:Ti films had lower surface roughness at high substrate temperature.

### 3.2. Optical properties

The optical energy gap $E_g$ could be obtained from the intercept of $(\alpha h\nu)^2$ versus $h\nu$ for direct allowed transitions [17]. Better linearity was observed for $(\alpha h\nu)^2$ versus $h\nu$ [17,18] as

Table 1
Deposition rate and elemental composition of $TiO_2$:Ti films with the sputtering conditions.

| DC power (W) | Substrate temperature (°C) | Deposition rate (Å/min) | O content (at.%) | Ti content (at.%) | O/Ti |
|---|---|---|---|---|---|
| 5 | 100 | 5.0 | 64.4 | 35.6 | 1.81 |
| 9 | 100 | 6.5 | 62.6 | 37.4 | 1.67 |
| 5 | 500 | 3.5 | 65.8 | 34.2 | 1.92 |
| 9 | 500 | 4.2 | 63.1 | 36.9 | 1.71 |

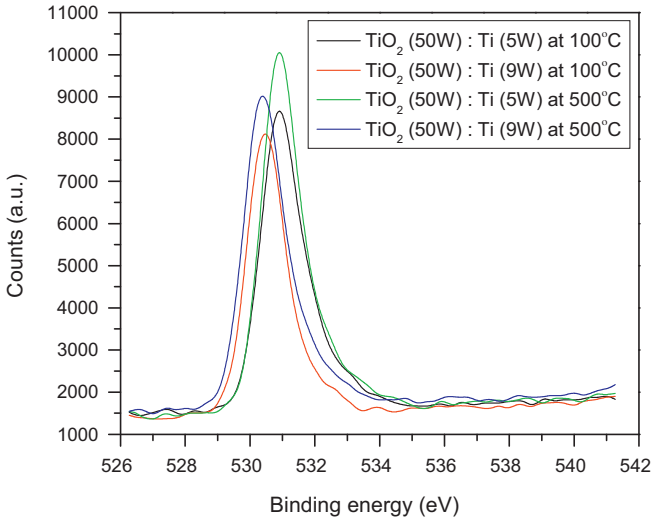


Fig. 2. O 1s photoelectron peak in the XPS spectrum of $TiO_2$:Ti films prepared at different dc powers and substrate temperatures.

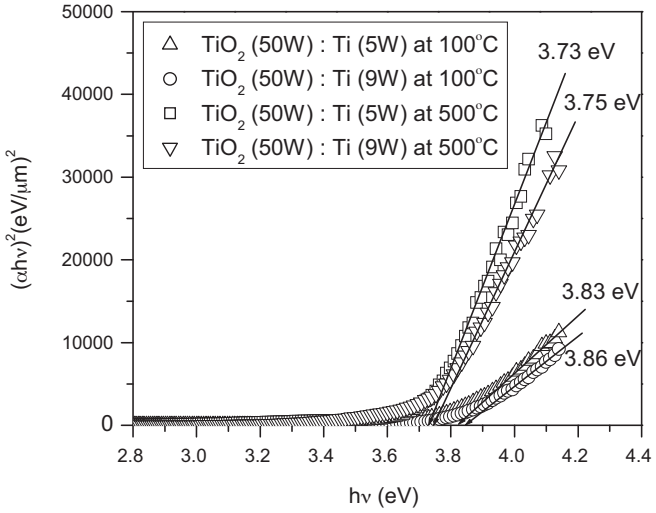


Fig. 4. Plots of $(\alpha h\nu)^2$ versus $h\nu$ for $TiO_2$:Ti films prepared at different dc powers and substrate temperatures.

shown in Fig. 4. Fig. 4 shows the plots of $(\alpha h\nu)^2$ versus $h\nu$ for $TiO_2$:Ti films prepared at different dc powers and substrate temperatures. The optical energy gap increased with the decrease of substrate temperature, but not evidently with the dc power. The change of optical energy gap after increasing substrate temperature has been interpreted as a Moss–Burstein shift, where the change is the result of a large decrease in the free carrier concentration, and the corresponding downward shift of the Fermi level to below the band edge [19,20].

Fig. 4 showed a low energy tail, which could be attributed to defects and impurities [21]. This abrupt energy gap extends to lower energies, due to the existence of structural defects and impurities within the material. The transitions via low-level impurities are responsible for this lower energy absorption region. Impurities in films are responsible for the low energy tail, called an impurity gap [22–24].

Fig. 5 shows the transmission in the UV–vis–IR region of $TiO_2$:Ti films prepared at different dc powers and substrate temperatures. In the near infrared region, the transmission of $TiO_2$:Ti films increased by decreasing substrate temperature, but not evidently by increasing dc power. The transmission in the visible region of $TiO_2$:Ti films prepared at 100 °C was lower. It was probably due to the relatively high surface roughness, which could result in more light scattering [25].

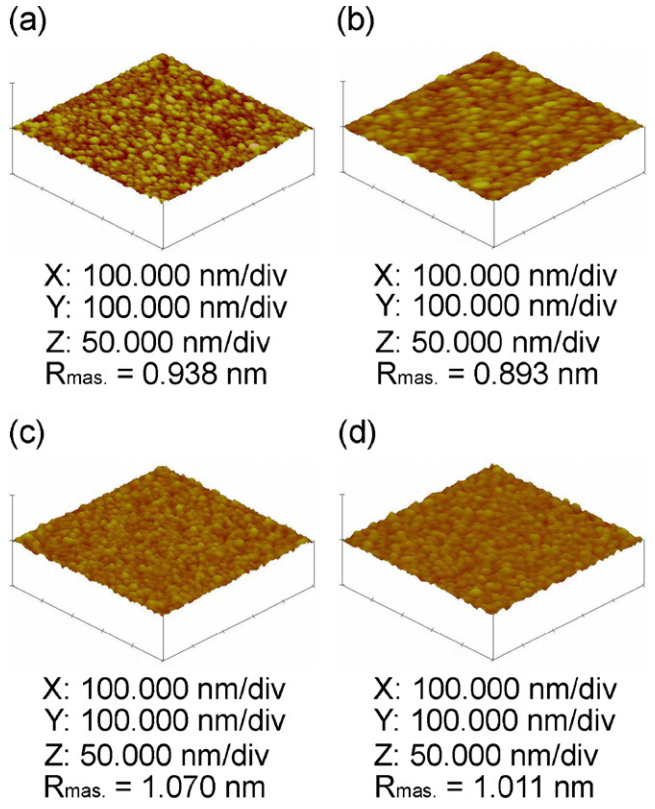


Fig. 3. The morphologies of $TiO_2$:Ti films deposited under different conditions. The dc power and substrate temperature are: (a) 5 W, 100 °C; (b) 5 W, 500 °C; (c) 9 W, 100 °C; and (d) 9 W, 500 °C.

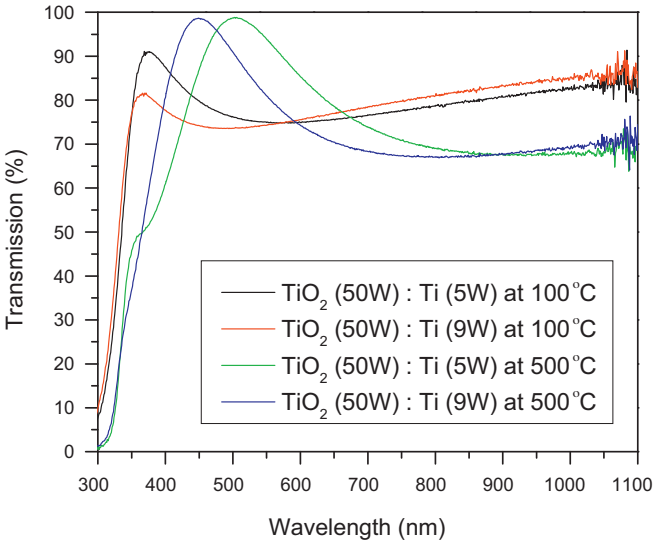


Fig. 5. The transmission in the UV–vis–IR region of $TiO_2$:Ti films prepared at different dc powers and substrate temperatures.

In addition, the transmission decreased substantially at short wavelengths near the ultraviolet range for $TiO_2$:Ti films prepared at different dc powers and substrate temperatures. By comparison, the absorption edge was observed at a slightly lower wavelength range for films deposited at lower substrate temperature. The shift of absorption edge may be attributed to the difference in optical energy gap. According to Figs. 4 and 5, the $TiO_2$:Ti films prepared at lower substrate temperature had relatively high energy gap, and this was probably why the blue shift of absorption edge occurred.

The index of refraction, $n$, which depends on the radiation intensity, may be expressed in terms of the nonlinear index $n_2$ ($cm^2\ W^{-1}$):

$$n(r,z) = n_0 + n_2 I(r,z) = n_0 + \Delta n(r,z) \tag{1}$$

where $n_0$ is the linear index of refraction, $I(r, z)$ is the irradiance of the laser beam within the sample, and $\Delta n(r, z)$ is the light-induced change in refractive index. Based on the assumption that a Gaussian beam is traveling in the $+z$ direction, the beam irradiance can be written as

$$I(r,z) = I_0 \frac{\omega_0^2}{\omega^2(z)} \exp\left[-\frac{2r^2}{\omega^2(z)}\right] \tag{2}$$

where $r$ is the radial radius of the imaginary sphere; $\omega_0$ is the spot size of the beam at the focus; $\omega(z) = \omega_0(1 + z^2/z_0^2)^{1/2}$ is the beam radius at a distance $z$ from the position of the waist; $z_0 = \pi\omega_0^2/\lambda$ is the diffraction length of the Gaussian beam, and $\lambda$ is the wavelength. The irradiance of the beam at the focus is denoted $I_0$ and in terms of the input laser power, $p_{in}$, equals $2p_{in}/\pi\omega_0^2$. Therefore, for a Gaussian laser beam, the radial dependence of the irradiance gives rise to a radially dependent parabolic refractive index change near the beam axis:

$$\Delta n(r,z) = n_2 I_0 \frac{\omega_0^2}{\omega^2(z)} \exp\left[-\frac{2r^2}{\omega^2(z)}\right]. \tag{3}$$

Moiré deflectometry is a sensitive technique for measuring changes in the refractive indices of materials. The sensitivity of this technique is determined by the minimum measurable-angle of rotation ($\alpha_{min}$). The tested sample was placed at various distances from the focal point of lens $L_1$, and the minimum angle of rotation was obtained. The same experiment was performed by using only a pure glass substrate to check the contribution of the glass substrate to the nonlinear refraction measurement. No observed fringe rotation or change in fringe size was found.

For the thin nonlinear medium of thickness $d$, the lowest nonlinear refractive index can be written as

$$n_{2,min} = \frac{\theta f_2^2}{z_t} \frac{\pi\omega_0^4}{d p_{in} z_0^2} \alpha_{min} \tag{4}$$

and the change in the minimum refractive index is

$$\Delta n_{min} = \frac{\omega_0^2 \theta f_2^2}{2 d z_t z_0^2} \alpha_{min}. \tag{5}$$

Fig. 6 shows the minimum nonlinear refractive indices and the change in the minimum refractive indices of $TiO_2$:Ti films deposited under different conditions. The nonlinear refraction indices were measured to be of the order of $10^{-8}\ cm^2\ W^{-1}$ and the changes in refractive indices were of the order of $10^{-5}$.

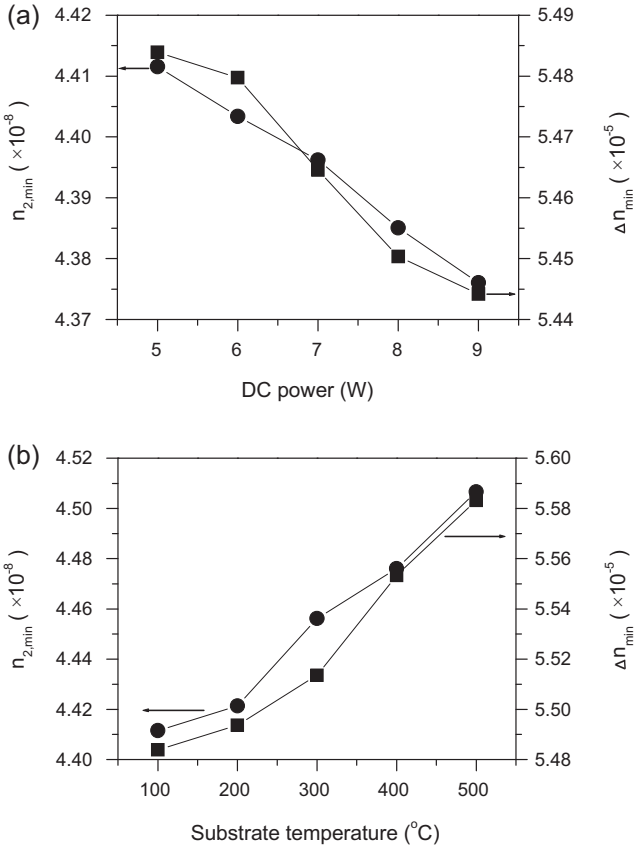


Fig. 6. The minimum nonlinear refractive indices and the change in the minimum refractive indices of $TiO_2$:Ti films deposited under different conditions. The dc power and substrate temperature are: (a) 5–9 W, 100 °C and (b) 5 W, 100–500 °C.

A change of the linear refractive index caused by stress is called the photoelastic effect [26]. The linear refractive index is specified by the indicatrix, which is an ellipsoid whose coefficients are the components of the relative dielectric impermeability tensor $B_{ij}$ at optical frequencies:

$$B_{ij} x_i x_j = 1. \tag{6}$$

The small change of the linear refractive index produced by stress is a small change in the shape, size and orientation of the indicatrix. This change is specified by the small changes in the coefficients $B_{ij}$.

If terms of higher-order than the first in the field of stresses are neglected, then the changes $\Delta B_{ij}$ in the coefficients are

$$\Delta B_{ij} = \varphi_{ijkl}\sigma_{kl} \quad \text{or} \quad \Delta B_{ij} = p_{ijrs}\varepsilon_{rs} \tag{7}$$

where $\varphi_{ijkl}$ and $p_{ijrs}$ are called the piezo-optical and strain-optical coefficients, which typically have the orders of magnitude of $10^{-12}$ and $10^{-1}\ Pa^{-1}$, respectively.

Based on the relation, $B = 1/n_0^2$, the change of linear refractive index for an isotropic film material is assumed to

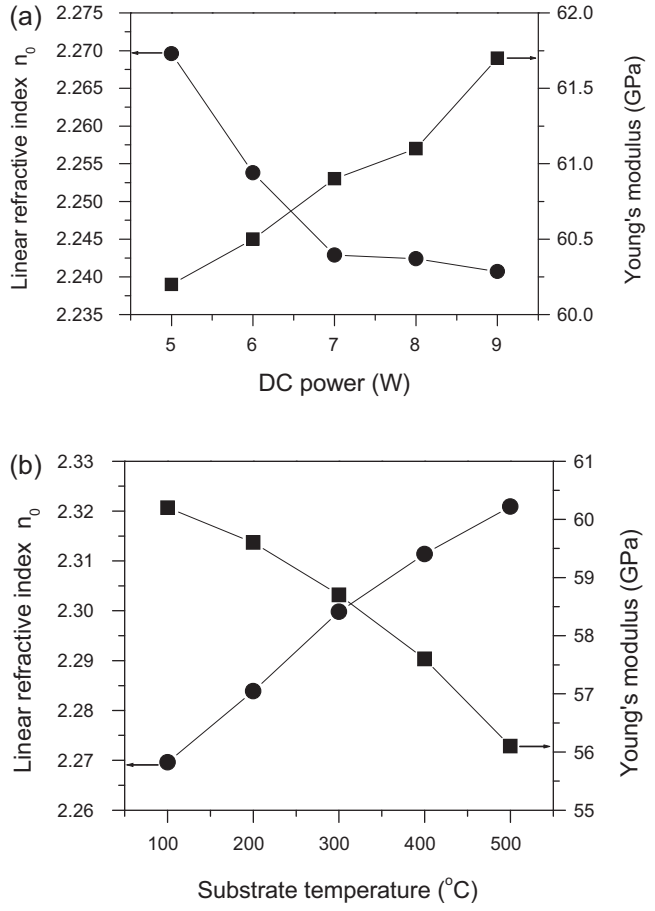


Fig. 7. The linear refractive indices and Young's moduli of $TiO_2$:Ti films deposited under different conditions. The dc power and substrate temperature are: (a) 5–9 W, 100 °C and (b) 5 W, 100–500 °C.

be [26,27]

$$\left(\frac{\partial n_0}{\partial \sigma}\right)_T = -\frac{1}{2} n_0^3 \varphi. \tag{8}$$

Consequently, a change in the linear refractive index due to film stress may affect the optical performance of an optical thin film, as shown in Eq. (8).

Fig. 7 shows the linear refractive indices and Young's moduli of $TiO_2$:Ti films deposited under different conditions. The linear refractive index $n_0$ of $TiO_2$:Ti film increased by decreasing dc power and increasing substrate temperature. However, the stress of $TiO_2$:Ti film decreased by decreasing dc power and increasing substrate temperature. The linear refractive index was found to correlate with the porosity [28,29]. It indicated that a dense $TiO_2$:Ti film with high linear refractive index and low stress could be obtained by decreasing dc power and increasing substrate temperature. The value of $\Delta n/\Delta\sigma$ is reportedly similar to the stress-optical coefficient [30]. The stress-optical coefficient, $(\partial n_0/\partial\sigma)_T$, of a $TiO_2$:Ti film was evaluated to be in the range of $-10.3 \times 10^{-12}$ to $-27.5 \times 10^{-12}\,\mathrm{Pa}^{-1}$.

## 4. Conclusions

When dc power increased, the $TiO_2$:Ti film had lower O/Ti atomic ratio and showed higher optical energy gap, especially at low substrate temperature. In the near infrared region, the transmission of $TiO_2$:Ti films increased by decreasing substrate temperature, but not evidently by increasing dc power. The optical transmission decreased substantially at short wavelengths near the ultraviolet range for films prepared at different dc powers and substrate temperatures. The nonlinear refraction indices of $TiO_2$:Ti films on the glass substrates were measured to be of the order of $10^{-8}\,\mathrm{cm}^2\,\mathrm{W}^{-1}$ and the changes in refractive indices were of the order of $10^{-5}$. By decreasing dc power and increasing substrate temperature, $TiO_2$:Ti film exhibited lower surface roughness, higher linear refractive index and lower stress-optical coefficient.

## Acknowledgment

The author would like to thank the National Science Council of the Republic of China, Taiwan, for financially supporting this research under Contract No. NSC-100-2221-E-260-014.

## References

[1] J. Robertson, Band offsets of wide-band-gap oxides and implications for future electronic devices, J. Vac. Sci. Technol. B 18 (2000) 1785–1791.
[2] B. O'Regan, M. Gratzel, A low-cost high-efficiency solar cell based on dye-sensitized colloidal $TiO_2$ films, Nature 353 (1991) 737–740.
[3] S. Takeda, S. Suzuki, H. Odaka, H. Hosono, Photocatalytic $TiO_2$ thin film deposited onto glass by DC magnetron sputtering, Thin Solid Films 392 (2001) 338–344.
[4] M. Okada, Y. Yamada, P. Jin, M. Tazawa, K. Yoshimura, Fabrication of multifunctional coating which combines low-e property and visible-light-responsive photocatalytic activity, Thin Solid Films 442 (2003) 217–221.
[5] S.S. Lin, J.L. Huang, D.F. Lii, Effect of substrate temperature on the properties of Ti-doped ZnO films by simultaneous rf and dc magnetron sputtering, Mater. Chem. Phys. 90 (2005) 22–30.
[6] W.T. Lim, C.H. Lee, Highly oriented ZnO thin films deposited on Ru/Si substrates, Thin Solid Films 353 (1999) 12–15.
[7] K.H. Yoon, J.W. Choi, D.H. Lee, Characteristics of ZnO thin films deposited onto Al/Si substrates by rf magnetron sputtering, Thin Solid Films 302 (1997) 116–121.
[8] M.J. Soileau, W.E. Williams, N. Mansour, E.W. Van Stryland, Laser-induced damage and the role of self-focusing, Opt. Eng. 28 (1989) 1133–1144.
[9] E.W. Van Stryland, Y.Y. Wu, D.J. Hagan, M.J. Soileau, K. Mansour, Optical limiting with semiconductors, J. Opt. Soc. Am. B 5 (1988) 1980–1988.
[10] M.J. Soileau, W.E. Williams, E.W. Van Stryland, Optical power limiter with picosecond response time, IEEE J. Quantum Electron. QE-19 (1983) 731–735.
[11] K. Mansour, M.J. Soileau, E.W. Van Stryland, Nonlinear optical properties of carbon-black suspensions (ink), J. Opt. Soc. Am. B 3 (1992) 1100–1109.
[12] Y. Zhang, G. Du, D. Liu, X. Wang, Y. Ma, J. Wang, J. Yin, X. Yang, X. Hou, S. Yang, Crystal growth of undoped ZnO films on Si substrates under different sputtering conditions, J. Cryst. Growth 243 (2002) 439–443.
[13] K. Koski, J. Hölsä, Pierre Juliet, Properties of aluminium oxide thin films deposited by reactive magnetron sputtering, Thin Solid Films 339 (1999) 240–248.
[14] C.D. Wagner, W.M. Riggs, L.E. Davis, J.F. Moulder, G.E. Muilenberg, Handbook of X-ray Photoelectron Spectroscopy, Perkin-Elmer Corporation, Eden Prairie, MN USA, 1979, p. 68.

[15] S.S. Lin, D.K. Wu, The properties of Al-doped $TiO_2$ nanoceramic films deposited by simultaneous rf and dc magnetron sputtering, Ceram. Int. 36 (2010) 87–91.
[16] D. Wang, U. Geyer, S. Schneider, G.V. Minnigerode, Grain sizes of Ni films measured by STM and X-ray methods, Thin Solid Films 292 (1997) 184–188.
[17] N. Serpone, D. Lawless, R. Khairutdinov, Subnanosecond relaxation dynamics in $TiO_2$ colloidal sols (particle sizes Rp = 1.0–13.4 nm). Relevance to heterogeneous photocatalysis, J. Phys. Chem. 99 (1995) 16655–16661.
[18] D.D. Claudio, A.R. Phani, S. Santucci, Enhanced optical properties of sol–gel derived $TiO_2$ films using microwave irradiation, Opt. Mater. 30 (2007) 279–284.
[19] B.E. Sernelius, K.F. Berggren, Z.C. Jin, I. Hamberg, C.G. Granqvist, Band-gap tailoring of ZnO by means of heavy Al doping, Phys. Rev. B 37 (1988) 10244–10248.
[20] E. Mollwo, in: R.G. Breckenridge, B.R. Russell, E.E. Hahn (Eds.), Proc. Photoconductivity Conf., Wiley, New York, 1954, p. 509.
[21] H. Demiryont, K.E. Nietering, Structure and optical properties of tin oxide films, Sol. Energy Mater. 19 (1989) 79–94.
[22] H. Demiryont, L.R. Thomson, G.J. Collins, Optical properties of aluminum oxynitrides deposited by laser-assisted CVD, Appl. Opt. 25 (1986) 1311–1318.
[23] M.L. Theye, Optical absorption in amorphous semiconductor films, Proc. SPIE 652 (1986) 146–152.
[24] S.S. Lin, J.L.Huang, Effect of thickness on the structural and optical properties of ZnO films by rf magnetron sputtering, Surf. Coat. Technol. 185 (2004) 222–227.
[25] T. Yamamoto, T. Shiosaki, A. Kawabata, Characterization of ZnO piezoelectric films prepared by rf planar-magnetron sputtering, J. Appl. Phys. 51 (6) (1980) 3113–3120.
[26] J.F. Nye, Physical Properties of Crystals: Their Representation by Tensors and Matrices, Oxford Science, New York, 1992.
[27] W. Lukosz, P. Pliska, Determination of thickness, refractive indices, optical anisotropy of and stresses in $SiO_2$ films on silicon wafers, Opt. Commun. 117 (1995) 1–7.
[28] G.S. Vicente, A. Morales, M.T. Gutierrez, Preparation and characterization of sol–gel $TiO_2$ antireflective coatings for silicon, Thin Solid Films 391 (2001) 133–137.
[29] S.S Lin, D.K. Wu, Enhanced optical properties of $TiO_2$ nanoceramic films by oxygen atmosphere, J. Nanosci. Nanotechnol. 10 (2010) 1099–1104.
[30] B. Hunsche, M. Vergöhl, H. Neuhäuser, F. Klose, B. Szyszka, T. Matthée, Effect of deposition parameters on optical and mechanical properties of MF- and DC-sputtered $Nb_2O_5$ films, Thin Solid Films 392 (2001) 184–190.